A Circularly-Polarized Metasurfaced Dipole Antenna with Wide Axial-Ratio Beamwidth and RCS Reduction Functions

Chen Chen[1], Zhuo Li[1, 2, *], Liangliang Liu[1], Jia Xu[1], Pingping Ning[1], Bingzheng Xu[1], Xinlei Chen[1], and Changqing Gu[1]

Abstract—A new circularly-polarized metasurfaced dipole antenna (MSDA) with wide axial-ratio (AR) beamwidth and radar cross section (RCS) reduction properties is proposed and studied in this paper. This antenna is a quite simple half-wavelength linear dipole right above a metasurface which consists of 9 double-head arrow-shaped unit cells arranged in a 3×3 layout. By cautiously choosing the geometrical parameters of the metasurface and tuning the distance between the dipole and the metasurface, the whole structure turns out to be a circularly-polarized antenna with RCS reduction feature. Simulation results show that the MSDA in circular polarization achieves an operating bandwidth of 410 MHz and a wide AR beamwidth of 123° and 90° in $\varphi = 0°$ and $\varphi = 90°$ planes respectively, together with a maximum RCS reduction of 10.4 dB in the whole operating band.

1. INTRODUCTION

Metamaterials, which are commonly composed of numerous electrically small scatterers arranged in a regular or irregular layout, are broadly defined as artificially homogeneous or inhomogeneous electromagnetic structures with unusual properties that are not available in nature [1–4]. Metasurface, a two-dimensional equivalent of metamaterial, has been attracting attention of researchers in the past few years. Due to its unique properties, metasurface has strong capability of manipulating electromagnetic waves, such as polarization conversion [5, 6], polarization rotation [7, 8] and wave redirection. Moreover, traditional antennas combined with metasurfaces, which can be referred to as metasurfaced antennas, can constitute new types of antenna with superior performance in return loss, polarization mode, radiation efficiency, gain value, low RCS, etc.. This brand new concept about antenna was first initiated by K. Chung, et al. in 2011. Conventional probe-fed microstrip patch antenna with a square-ring type metasurface loaded was proposed to show simultaneous enhancement on impedance bandwidth, broadside emission, and antenna efficiency [9]. From then on, researches on metasurfaced antenna have been springing up in a rash. A thin metasurface was loaded onto a circularly-polarized slot antenna and backed by a metallic reflector at close distance to achieve a high front-to-back radiation ratio [10]. A new ultra-thin directional broadband antenna using a nonuniform aperiodic metasurface was introduced in [11]. A stacked patch antenna using a two-layered metasurface was designed to achieve RCS reduction [12]. A wide-band and low-profile circularly-polarized antenna using metasurface for WLAN or satellite communication application was proposed in [13]. As a whole, an increasing number of potential applications using metasurfaces are explored in the microwave, terahertz and optical regime.

Circularly-polarized antennas play important roles in RFID, radar, WLAN, satellite communication and sensor system because of their stability in signal reception and smashing mobility [14]. Based on the design of a metamaterial reflective surface presented in [15], analogous metasurface whose unit

cell consists of a rectangular loop with a diagonal microstrip was placed close to a source antenna to convert the linearly polarized signal generated from the source into a circularly polarized one [16, 17]. Broadband circular and linear polarization conversion has been reported by using thin birefringent reflective metasurfaces, which are composed of two orthogonal I-shaped structures placed on a substrate with a grounded sheet [18]. Studies have shown that circular polarization, especially broadband circular polarization, is relatively easy to implement with the use of metasurfaces, but wide AR beamwidth and low RCS properties are seldom investigated.

In this paper, we intend to utilize the metasurface proposed in [5], which was in fact the shear deformation of that used in [10, 15–17], to design a circularly polarized antenna and mainly focus on the wide AR beamwidth and RCS reduction performances. In order to make the designed antenna work in C-band for satellite communications, the geometrical parameters of the metasurface used in [5] are redesigned. Then a simple dipole antenna is selected as the source and placed above the metasurface as shown in Figs. 1(a) and (b) to obtain circularly polarized radiation. Through simulations and optimizations, a circularly-polarized MSDA with wide AR beamwidth is obtained and the angular region can be up to $123°$ ($\varphi = 0°$ plane) and $90°$ ($\varphi = 90°$ plane) in the two principle planes. In addition, this antenna can also realize a RCS reduction of more than $7\,\text{dB}$ in almost the whole operating band in comparison with the non-metasurfaced dipole antenna (non-MSDA, the same dipole combined with a same-sized copper plate that is in the same position with the metasurface), exhibiting great potentials in microwave applications.
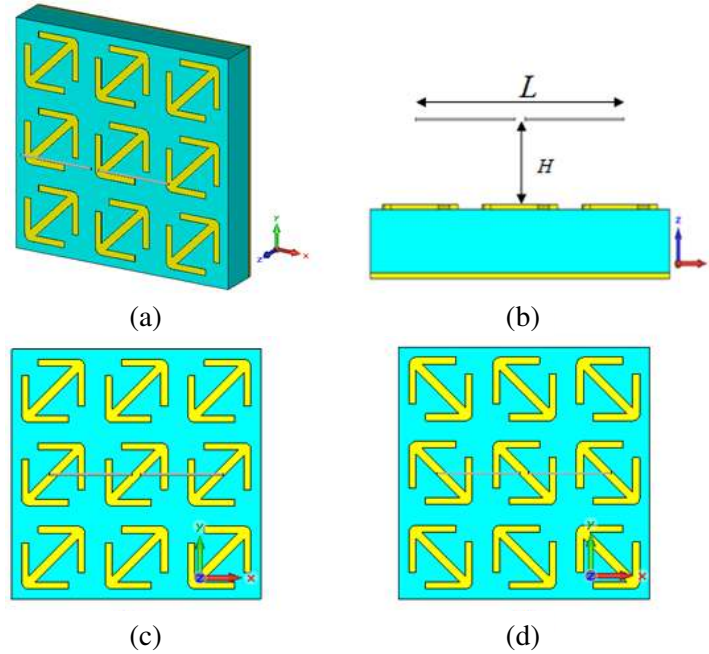

(a)   (b)

(c)   (d)

Figure 1. Geometry of the proposed MSDA, (a) three-dimensional view, (b) front view, top view of the (c) LHCP MSDA and (d) RHCP MSDA.

2. DESIGN AND ANALYSIS

The MSDA proposed here is composed of a simple dipole antenna (as the source antenna) and a metasurface as shown in Fig. 1(a). Fig. 2 shows the geometry of the unit cell designed for the metasurface. Each unit cell consists of a double-head arrow resonator that is placed on the top of the F4B-2 substrate (with the relative permittivity $\varepsilon_r = 2.65$, the loss tangent $\tan \delta = 0.001$) backed with a copper ground. The thickness of the substrate and the metallic patterns are $h = 6\,\text{mm}$ and $t = 0.018\,\text{mm}$ respectively as shown in Fig. 2(a). The dimensions of the unit cell specified in Fig. 2(b) are $p = 12\,\text{mm}$, $l = 10\,\text{mm}$, $d = 5.7\,\text{mm}$, $w = 1.2\,\text{mm}$ and $g = 1\,\text{mm}$. This proposed MSDA is designed
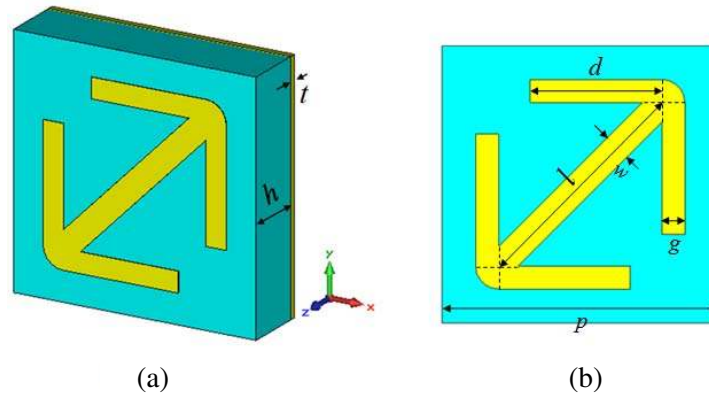
(a)   (b)

Figure 2. Geometry of the metasurface unit cell with specified parameters, (a) three-dimensional view, (b) top view.
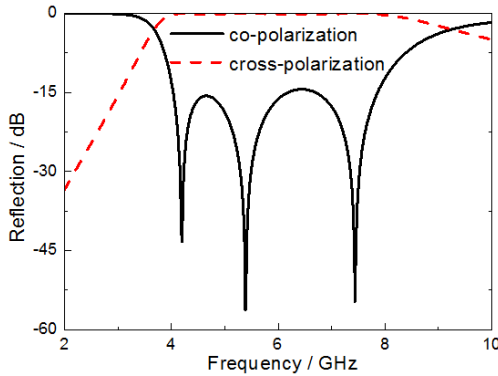

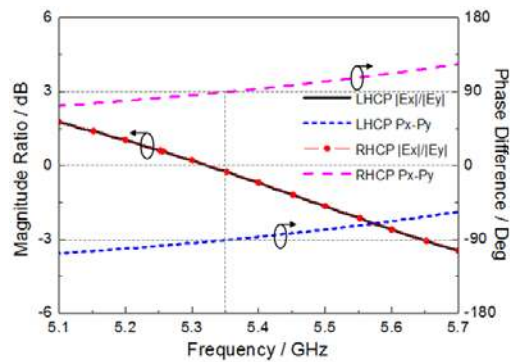**Figure 3.** Co- and cross-polarization reflection of the metasurface.

Figure 4. The magnitude ratio and phase difference between two orthogonal components (Ex and Ey) of the total electric fields above the dipole in the far-field boresight ($+z$) direction.

here for C-band satellite communication applications, however, the operating band can be tuned by scaling the geometrical parameters of the metasurface.

The metasurface can realize ultra-wideband polarization conversion in the microwave regime through multiple plasmon resonances. In order to verify this property, full wave simulations are performed in the commercial software CST Microwave Studio with the Frequency Domain Simulator. Fig. 3 shows the co- and cross-polarization reflection versus frequency. The co-polarization reflection is below -15 dB in almost all the C-band and the cross-polarization reflection is nearly 0 dB, which indicates the linear polarization mode can be changed with high efficiency in the C-band. With respect to the principle of polarization conversion, Ref. [5] gives a detailed theoretical analysis. In our case, we take advantage of the metasurface to realize polarization conversion of the reflected wave, accordingly the reflected wave and the directed wave emitted from the dipole antenna will generate two orthogonal polarization waves. Then circularly polarized wave can be possibly generated when the dipole is placed at a certain height above the metasurface.

The metasurface used in the proposed MSDA consists of 9 aforementioned unit cells in a 3×3 arrangement. A dipole antenna is placed along the x-axis above the metasurface center with the height H and length of $L = 25$ mm as shown in Fig. 1(b). Consequently, x-polarized radiated wave toward the negative direction of z-axis is generated and almost totally reflected by the metasurface and converted to its orthogonal polarized wave (y-polarized wave) towards z-axis. Since the radiated wave toward the positive direction of z-axis is still x-polarized, the directed wave (x-polarized along $+z$ axis) and the

reflected wave (y-polarized along $+z$ axis) will bring about circularly polarized wave when they have a phase difference of $\pm 90°$. The phase difference is closely related to the perpendicular distance H between the dipole and the metasurface, marked in Fig. 1(b). In theory, wave path-difference of one-quarter-wavelength will result in a phase difference of $\pm 90°$. As a consequence, when H approximately equals to $7\,\text{mm}$ ($\lambda_0/8$), the phase difference between the direct and the reflected wave will be $\pm 90°$ and circularly polarized radiation will come into being. However, the proposed metasurface is in the near-field regions of source antenna in our case, which is very different from the situation of plane wave irradiating. In order to obtain satisfactory performance, parameter sweep for H is carried out in CST Microwave Studio and preferable circular polarization can be realized in a relatively wide band when $H = 8\,\text{mm}$.

In order to directly show the performance of circular polarization, we utilize the farfield probe in CST Microwave Studio to obtain the magnitude and phase of two orthogonal components of the electric fields (Ex and Ey) in the farfield boresight ($+z$) direction of the proposed MSDA whose top view is shown in Fig. 1(c). Fig. 4 shows the phase difference and magnitude ratio between $|Ex|$ and $|Ey|$. It is observed that the magnitude ratio ($|Ex|/|Ey|$) is between $\pm 3\,\text{dB}$ and the phase difference (Phase(Ex)-Phase(Ey)) is about $-90°$ around the center frequency ($f_0 = 5.35\,\text{GHz}$). In this case, the total electric fields above the dipole can become the circularly polarized wave, which is just a left-handed circular polarization (LHCP) due to the phase of Ex lagging phase of Ey about $90°$. Counterclockwise rotating the double-head arrow resonator atop the metasurface around the center as shown in Fig. 1(d), the resultant electric fields will be the right-handed circularly polarized (RHCP) wave due to the phase of Ex leading phase of Ey about $90°$. It can also be observed in Fig. 4 that the magnitude ratio of the RHCP antenna is the same as that of the LHCP one.

3. SIMULATION RESULTS

Performance evaluation of the proposed MSDA is accomplished with the help of simulations. Operating bandwidth, gain, radiation patterns, wide AR beamwidth and RCS reduction are discussed in detail as follows. In view of the fact that simulation results about above parameters of the LHCP and RHCP MSDA are identical except the circular polarization mode (reflected by radiation patterns as shown in Fig. 6), we only give the simulated results of the LHCP MSDA.

3.1. Operating Bandwidth and Gain

Figure 5(a) shows the S_{11} parameters of the proposed MSDA compared with the non-MSDA. It can be seen that the simulated return loss bandwidth of the MSDA is $810\,\text{MHz}$ varied from $4.89\,\text{GHz}$ to $5.7\,\text{GHz}$, which is wider than that of the non-MSDA, about $210\,\text{MHz}$ from $4.85\,\text{GHz}$ to $5.06\,\text{GHz}$. Nevertheless,
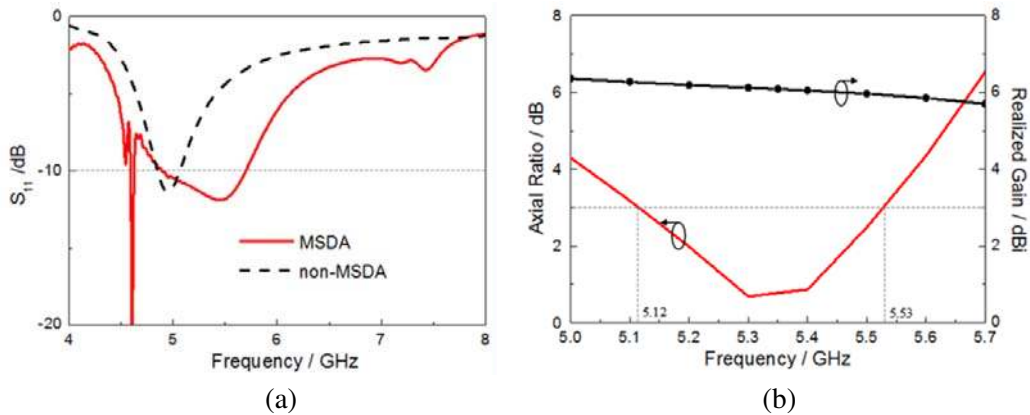

Figure 5. Simulated reflection coefficient S_{11}, AR bandwidth and gain characteristics, (a) S_{11} versus frequency of the MSDA and non-MSDA, (b) axial ratio and realized gain versus frequency of the MSDA.

the designed metasurfaced antenna is committed to realize circular polarization, so the AR bandwidth (AR < 3 dB) should also be taken into account when evaluating the operating bandwidth. Fig. 5(b) shows the simulated frequency responses of the AR in the boresight (along $+z$ axis). The AR bandwidth is 410 MHz varied from 5.12 to 5.53 GHz, within the interval of return loss bandwidth, which determines the operating bandwidth. Moreover, the realized gain of the MSDA is higher than that of traditional dipole antenna. As is shown in Fig. 5(b), the maximum gain of the MSDA in the operating band is 6.25 dBi.

3.2. Radiation Pattern and Wide AR Beamwidth

As shown in Fig. 4, the magnitude ratio ($|Ex|/|Ey|$) and phase difference (Phase(Ex)-Phase(Ey)) of the LHCP and RHCP MSDA is nearly 0 dB and $\mp 90°$ respectively when $f_0 = 5.35$ GHz, indicating the most excellent performance of circular polarization, namely the minimum AR in the boresight (along $+z$ axis), will be obtained at this frequency. Fig. 6 shows the simulated radiation patterns of the LHCP and RHCP MSDA in the $\varphi = 0°$ and $\varphi = 90°$ planes at the center frequency 5.35 GHz. It can be seen that the LHCP fields are about 37 dB stronger than the RHCP fields in the boresight ($+z$) direction of the LHCP MSDA while the result of the RHCP MSDA turns out to be just the reverse for both planes. Radiation patterns demonstrate superb performance of circular polarization at 5.35 GHz, but this does not mean the angular region of circular polarization is widest at this frequency. Simulation results show that the AR beamwidth is relatively wider when $f = 5.5$ GHz, may be wider at other precise frequency we do not scan. Fig. 7 shows the AR characteristic of the proposed MSDA in the boresight at the frequency $f = 5.5$ GHz. Here we only consider two principal planes ($\varphi = 0°$ and $\varphi = 90°$ planes), which are xz-plane and yz-plane as shown in Fig. 1(a). The angle range in which AR is less than 3 dB in two orthogonal planes is 123° ($\varphi = 0°$ plane) and 90° ($\varphi = 90°$ plane), showing great circular polarization performance of wide AR beamwidth.

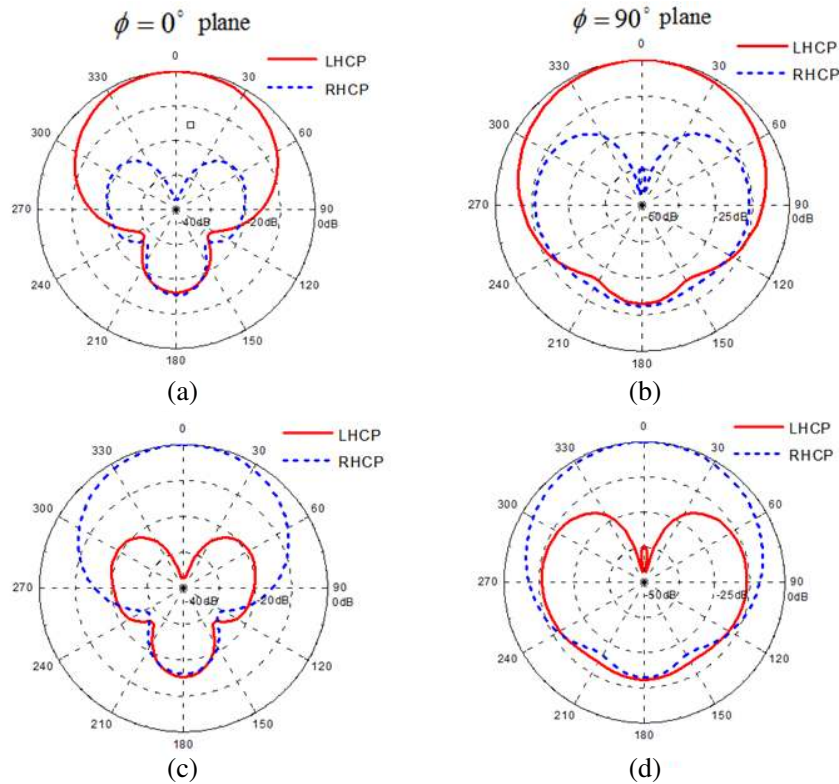**Figure 6.** Radiation patterns of the proposed LHCP and RHCP MSDA in $\varphi = 0°$ and $\varphi = 90°$ planes at the frequency $f = 5.35$ GHz, (a) LHCP MSDA in $\varphi = 0°$ plane, (b) LHCP MSDA in $\varphi = 90°$ plane, (c) RHCP MSDA in $\varphi = 0°$ plane, (d) RHCP MSDA in $\varphi = 90°$ plane.

3.3. RCS Reduction

In radio frequency stealth applications, RCS is a vital factor, and RCS reduction is of great importance in the antenna design. Fig. 8 shows the simulated mono-static RCS of the MSDA and non-MSDA, and the difference (depicted by the blue line) between them is shown in the same graph. It shows that the RCS of the non-MSDA is varied from -19.1 dBsm to -18.5 dBsm between 5 and 6 GHz, while the proposed MSDA makes the RCS dramatically reduced in the simulation spectrum. It can be seen that the MSDA can obtain a RCS reduction of more than 7 dB, and the maximum reduction can be up to 10.4 dB in the operating band of 5.12 to 5.53 GHz.
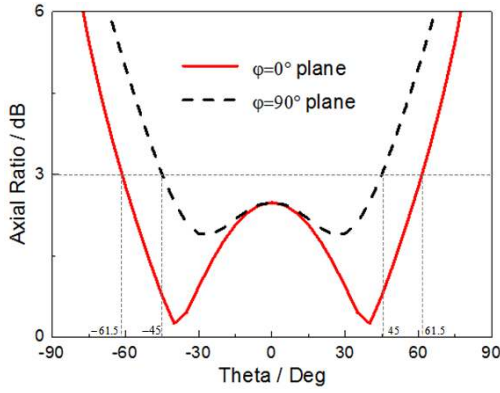

Figure 7. AR characteristic of $\varphi = 0°$ and $\varphi = 90°$ planes in the boresight $(+z)$ direction of the MSDA at the frequency $f = 5.5$ GHz.
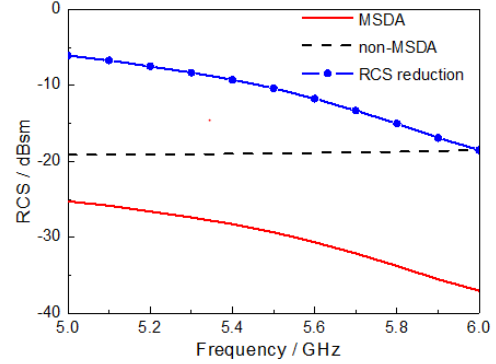

Figure 8. Simulated RCS for a normal incident plane wave with x-polarization on the MSDA and non-MSDA together with the RCS difference between them.

4. CONCLUSION

In this paper, a new circularly-polarized MSDA with wide AR beamwidth and RCS reduction functions is proposed using cautiously designed metasurface composed of 9 double-head arrow-shaped unit cells arranged in a 3×3 layout. This metasurface is committed to realize polarization conversion with high efficiency and can be widely applied at different microwave frequencies by scaling the geometrical parameters of the unit cell. Simulation results show that the MSDA in circular polarization achieves an effective operating bandwidth of 410 MHz and a wide AR beamwidth of 123° ($\varphi = 0°$ plane) and 90° ($\varphi = 90°$ plane) in the two principle planes. Moreover, the proposed MSDA can obtain a maximum RCS reduction of 10.4 dB in the whole operating band compared with the non-MSDA. This designed antenna can be widely applied in satellite communication, RFID, radar system, etc.

REFERENCES

1. Caloz, C. and T. Itoh, *Electromagnetic Metamaterials: Transmission Line Theory and Microwave Applications*, New Jersey, John Wiley & Sons, Hoboken, 2005.

2. Chin, J. Y., M. Lu, and T. J. Cui, "Metamaterial polarizers by electric-field-coupled resonators," *Applied Physics Letters*, Vol. 93, No. 25, 251903, 2008.

3. Holloway, C. L., A. Dienstfrey, E. F. Kuester, J. F. O'Hara, A. K. Azad, and A. J. Taylor, "A discussion on the interpretation and characterization of metafilms/metasurfaces: The two-dimensional equivalent of metamaterials," *Metamaterials*, Vol. 3, No. 2, 100–112, 2009.

4. Holloway, C. L., E. F. Kuester, J. A. Gordon, J. O'Hara, J. Booth, and D. R. Smith, "An overview of the theory and applications of metasurfaces: The two-dimensional equivalents of metamaterials," *IEEE Antennas and Propagation Magazine*, Vol. 54, No. 2, 10–35, 2012.

5. Chen, H. Y., J. F. Wang, H. Ma, S. B. Qu, Z. Xu, A. X. Zhang, M. B. Yan, and Y. F. Li, "Ultra-wideband polarization conversion metasurfaces based on multiple plasmon resonances," *Journal of Applied Physics*, Vol. 115, No. 15, 154504, 2014.

6. Chen, H. Y., H. Ma, S. B. Qu, J. F. Wang, Y. F. Li, H. Y. Yuan, and Z. Xu, "Ultra-wideband polarization conversion metasurfaces," *2014 3rd Asia-Pacific Conference on Antennas and Propagation (APCAP)*, 1009–1011, 2014.

7. Zhang, W., W. M. Zhu, E. E. M. Chia, Z. X. Shen, H. Cai, Y. D. Gu, W. Ser, and A. Q. Liu, "A pseudo-planar metasurface for a polarization rotator," *Optics Express*, Vol. 22, No. 9, 10446–10454, 2014.

8. Caputo, J. G., I. Gabitov, and A. I. Maimistov, "Polarization rotation by an rf-SQUID metasurface," *Physical Review B*, Vol. 91, No. 11, 115430, 2015.

9. Chung, K. L. and S. Chaimool, "Diamagnetic metasurfaces for performance enhancement of microstrip patch antennas," *Proceedings of the 5th European Conference on Antennas and Propagation (EUCAP)*, 48–42, 2011.

10. Chung, K. L. and S. Kharkovsky, "Metasurface-loaded circularly-polarized slot antenna with high front-to-back ratio," *Electronics Letters*, Vol. 49, No. 16, 979–981, 2013.

11. Chamok, N., T. K. Anthony, S. J. Weiss, and M. Ali, "Ultra-thin UHF broadband antenna on a non-uniform aperiodic (NUA) metasurface," *IEEE Antennas and Propagation Magazine*, Vol. 57, No. 2, 167–180, 2015.

12. Huang, C., W. B. Pan, X. L. Ma, and X. G. Luo, "Wideband radar cross-section reduction of a stacked patch array antenna using metasurface," *IEEE Antennas and Wireless Propagation Letters*, Vol. 14, 1369–1372, 2015.

13. Wu, Z., H. X. Liu, Y. Shi, and L. Li, "Metamaterial-inspired wideband low-profile circularly polarized antenna," *2015 IEEE International Conference on Computational Electromagnetics (ICCEM)*, 45–46, 2015.

14. Rao, B. R., W. Kunysz, R. Fante, and K. McDonald, *GPS/GNSS Antennas*, Artech House, Norwood, MA, USA, 2013.

15. Chaimool, S., K. L. Chung, and P. Akkaraekthalin, "Simultaneous gain and bandwidths enhancement of a single-feed circularly polarized patch antenna using a metamaterial reflective surface," *Progress In Electromagnetics Research B*, Vol. 22, 23–37, 2010.

16. Zhu, H. L., K. L. Chung, X. L. Sun, S. W. Cheung, and T. I. Yuk, "CP metasurfaced antennas excited by LP sources," *IEEE Antennas and Propagation Society International Symposium (APSURSI)*, 1–2, 2012.

17. Zhu, H. L., S. W. Cheung, K. L. Chung, and T. I. Yuk, "Linear-to-circular polarization conversion using metasurface," *IEEE Transactions on Antennas and Propagation*, Vol. 61, No. 9, 4615–4623, 2013.

18. Ma, H. F., G. Z. Wang, G. S. Kong, and T. J. Cui, "Broadband circular and linear polarization conversions realized by thin birefringent reflective metasurfaces," *Optical Materials Express*, Vol. 4, No. 8, 1717–1724, 2014.